Antitumor activity of luteolin in human colon cancer SW620 cells is mediated by the ERK/FOXO3a signaling pathway

Potočnjak, Iva; Šimić, Lidija; Gobin, Ivana; Vukelić, Iva; Domitrović, Robert

Source / Izvornik: **Toxicology in Vitro, 2020, 66**

Journal article, Accepted version
Rad u časopisu, Završna verzija rukopisa prihvaćena za objavljivanje (postprint)

https://doi.org/10.1016/j.tiv.2020.104852

Permanent link / Trajna poveznica: https://urn.nsk.hr/urn:nbn:hr:184:895251

Journal Pre-proof

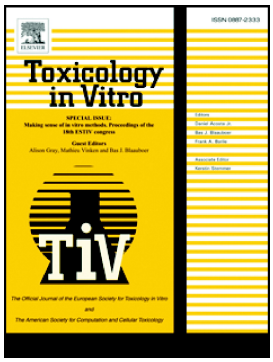

Antitumor activity of luteolin in human colon cancer SW620 cells is mediated by the ERK/FOXO3a signaling pathway

Iva Potočnjak, Lidija Šimić, Ivana Gobin, Iva Vukelić, Robert Domitrović

PII: S0887-2333(19)30924-5

DOI: https://doi.org/10.1016/j.tiv.2020.104852

Reference: TIV 104852

To appear in: *Toxicology in Vitro*

Received date: 11 December 2019

Revised date: 3 April 2020

Accepted date: 3 April 2020

Please cite this article as: I. Potočnjak, L. Šimić, I. Gobin, et al., Antitumor activity of luteolin in human colon cancer SW620 cells is mediated by the ERK/FOXO3a signaling pathway, *Toxicology in Vitro* (2020), https://doi.org/10.1016/j.tiv.2020.104852

Antitumor activity of luteolin in human colon cancer SW620 cells is mediated by the ERK/FOXO3a signaling pathway

Iva Potočnjak[a], Lidija Šimić[a], Ivana Gobin[b], Iva Vukelić[a], Robert Domitrović[a*]

[a]Department of Medical Chemistry, Biochemistry and Clinical Chemistry, Faculty of Medicine, University of Rijeka, Rijeka, Croatia

[b]Department of Microbiology and Parasitology, Faculty of Medicine, University of Rijeka, Rijeka, Croatia

[*]**Correspondence**: Prof. Robert Domitrović, Department of Medical Chemistry, Biochemistry and Clinical Chemistry, Faculty of Medicine, University of Rijeka, B. Branchetta 20, 51000 Rijeka, Croatia. E-mail: robert.domitrovic@uniri.hr.

Abstract

The aim of this study was to investigate the mechanism of the anticancer activity of luteolin in metastatic human colon cancer SW620 cells. Luteolin dose-dependently reduced the viability and proliferation of SW620 cells and increased the expression of antioxidant enzymes. The expression of antiapoptotic protein Bcl-2 decreased whereas the expression of proapoptotic proteins Bax and caspase-3 increased by luteolin treatment, resulting in increased poly (ADP-ribose) polymerase (PARP) cleavage and terminal deoxynucleotidyl transferase dUTP nick end labeling (TUNEL) positivity. Luteolin also increased the expression of autophagic proteins Beclin-1, autophagy-related protein 5 (Atg5) and microtubule-associated protein 1A/1B-light chain 3 beta-I/II (LC3B-I/II), while the usage of 3-methyladenine suggested a prosurvival role of autophagy. Moreover, treatment with luteolin induced reversal of the epithelial-mesenchymal transition process through the suppression of the wingless-related integration site protein (Wnt)/β catenin pathway. The cytotoxic activity of luteolin coincided with the activation of extracellular signal-regulated kinase 1/2 (ERK1/2) and forkhead box O3a (FOXO3a). Treatment with the mitogen-activated protein kinase kinase (MEK) inhibitor PD0325901 inhibited ERK-dependent FOXO3a phosphorylation, resulting in increased FOXO3a expression and apoptosis, with the suppression of autophagy. The results of the current study suggest the antitumor activity of luteolin in SW620 cells through the ERK/FOXO3a-dependent mechanism, as well as its antimetastatic potential.

Keywords: colon cancer SW620 cells; luteolin; mitogen-activated protein kinase; forkhead box O3a; apoptosis; autophagy.

Abbreviations: 3-MA, 3-methyladenine; AO, acridine orange; ATCC, American Type Culture Collection; Atg, autophagy-related protein; BCA, bicinchoninic acid; Bcl-2; B-cell lymphoma 2; BSA, bovine serum albumin; DAPI, 4',6-diamidino-2-phenylindole; DMEM, Dulbecco's modified Eagle's medium; DMSO, dimethyl sulfoxide; ECL, enhanced chemiluminescence; EDTA, ethylenediaminetetraacetic acid; EMT, epithelial–mesenchymal transition; ERK1/2, extracellular signal-regulated kinase 1/2; FBS, fetal bovine serum; FOXO3a, forkhead box O3a; 5-fluorouracil (5-FU); HO-1, heme oxygenase-1; HRP, horseradish peroxidase; IC_{50}, 50% inhibitory concentration; JNK1/2, c-Jun N-terminal kinase 1/2; LC3B-I/II, microtubule-associated protein 1A/1B-light chain 3 beta-I/II; MAPK, mitogen-activated protein kinase; MEK, mitogen-activated protein kinase kinase; PARP, poly (ADP-ribose) polymerase; PBS, phosphate buffered saline; PI, propidium iodide; POD, peroxidase; PVDF, polyvinylidene fluoride; RIPA, radioimmunoprecipitation assay; ROS, reactive oxygen species; SDS, sodium dodecyl sulphate; SDS-PAGE, SDS-polyacrylamide gel electrophoresis; SOD2, superoxide dismutase; TBS, Tris-buffered saline; Tris, tris(hydroxymethyl)aminomethane, TUNEL, terminal deoxynucleotidyl transferase dUTP nick end labeling; Wnt, Wingless-related integration site protein; XTT, 2,3-bis(2-methoxy-4-nitro-5-sulfophenyl)-2H-tetrazolium-5-carboxanilide.

1 **Introduction**

Colorectal cancer is one of the most common malignancies in humans, resulting in the fourth most cancer-related death worldwide (Bi et al., 2018; Siegel et al., 2017). Metastasis, which occurs in advanced stages of cancer, is considered as the most life-threatening event in patients with cancer (Kalluri and Weinberg, 2009). Colon cancer survival is closely related to tumor stage, rapidly decreasing in individuals with metastatic disease. Since metastasis accounts for over 90% of colon cancer deaths, therapies that target this process and block disease progression are of major concern (Hewitt et al., 2000). Human colon carcinoma SW620 cell line is derived from a secondary colon tumor and represents a valuable resource for examining the late stage in colon cancer progression (Hewitt et al., 2000).

Phytochemicals play an important role in the development of anticancer agents (Newman & Cragg, 2016). In human colorectal cancer, many of these natural compounds exhibited antiproliferative and cytotoxic activity, emerging as promising candidates for its treatment (Redondo-Blanco, Fernandez, Gutierrez-Del-Rio, Villar, & Lombo, 2017). Recent studies indicated that phytochemicals could exhibit anticancer effects, not only in primary but also in metastatic colon cancer cells. For instance, urolithin A, a major ellagitannin metabolite, was shown to induce autophagy and inhibit metastatic potential of SW620 cells (Zhao et al., 2018). Another compound, a bisbenzylisoquinoline alkaloid tetrandrine, suppressed adhesion, migration, and invasion of SW620 cells via inhibition of nuclear factor-kappa B and matrix metalloproteinases (Juan et al., 2018). Kustiawan et al. (2017) showed the antiproliferative activity of cardol, alkyl resorcinol found in propolis, in SW620 cells. However, the mechanism of anticancer activity of phytochemicals in metastatic

colorectal carcinoma has been poorly studied. The extracellular signal-regulated kinase 1/2 (ERK1/2) and forkhead box O (FOXO) pathways were shown to play a critical role in the development and progression of cancer (Dhillon, Hagan, Rath, & Kolch, 2007). ERK can phosphorylate and activate numerous targets orchestrating a complex cellular response that is frequently pro-proliferative (Brandt et al., 2019). Among them, FOXOs acts as mediators of the tumor response to various therapies (Coomans de Brachène & Demoulin, 2016; Fernández de Mattos, Villalonga, Clardy, & Lam, 2008). Understanding the nature of activation of signaling pathways in each tumor type is crucial in developing therapy regimens because different tumors have unique mechanisms of cell signaling (Burotto, Chiou, Lee, & Kohn, 2014).

The flavone luteolin (3',4',5,7-tetrahydroxyflavone), a member of the flavonoid family, can be found in various edible and medicinal plants in glycosylated forms and as an aglycone (Shimoi et al., 1998). Numerous studies showed that luteolin possesses many beneficial effects both *in vitro* and *in vivo*, including anti-oxidant and anti-inflammatory activity (Seelinger, Merfort, & Schempp, 2008). Previously, we showed the hepatoprotective and renoprotective activity of luteolin against chemically-induced injury in mice (Domitrovic et al., 2013; Domitrovic, Jakovac, Tomac, & Sain, 2009). Luteolin also exhibited anticancer action in a variety of human cancer cells by aiming multiple molecular targets (Tuorkey, 2016). It also blocks cancer development *in vitro* and *in vivo* by activation of cell cycle arrest, inhibition of proliferation of cancer cells, protection from carcinogenic stimuli, and by inducing apoptosis through different signaling pathways (Imran et al., 2019). However, the cytotoxic activity of luteolin in metastatic human colon cancer and the role of ERK/FOXO3a in its anticancer activity was not previously studied.

In the current study, we investigated the molecular mechanisms of antiproliferative, cytotoxic, and antimetastatic activity of luteolin in human colon carcinoma SW620 cells.

2 Materials and methods

2.1 Chemicals

Luteolin (97%) was obtained from Alfa Aesar (Ward Hill, MA, USA). Dimethyl sulfoxide (DMSO), sodium dodecyl sulfate (SDS), bovine serum albumin (BSA, fraction V, 99%), and tris(hydroxymethyl)aminomethane (Tris 99%) were purchased from Sigma-Aldrich (Steinheim, Germany). Acridine orange (AO), Tween-80, Mowiol 4-88, and acrylamide/bisacrylamide solution 40% were purchased from Carl Roth GmbH (Karlsruhe, Germany). Fluorescent stain 4',6-diamidino-2-phenylindole (DAPI) was from Invitrogen, Thermo Fischer Scientific (Carlsbad, CA, USA). Amersham Hybond-P polyvinylidene fluoride (PVDF) blotting membrane was from GE Healthcare Life Sciences (Buckinghamshire, United Kingdom). Non-fat dry milk was purchased from Biorad (Hercules, CA, USA). Radioimmunoprecipitation assay (RIPA) buffer (sc-24948) and antibodies against caspase-3 p11 (sc-271759), autophagy-related protein 7 (Atg7) (sc-376212), wingless-related integration site protein 3 (Wnt3) (sc-74537), and Beclin-1 (cs-48341) were from Santa Cruz Biotechnology (Santa Cruz, CA, USA). Mouse monoclonal antibody beta-actin (β-actin) (ab8226), rabbit monoclonal antibodies to Bax (ab32503), superoxide dismutase (SOD2) (ab13533), B-cell lymphoma 2 (Bcl-2) (ab7973), p21 (ab109199), heme oxygenase-1 (HO-1) (ab13243), and microtubule-associated protein 1A/1B-light chain 3 beta-I/II (LC3B-I/II) (ab48394) were purchased from Abcam (Cambridge, UK). XTT Cell Viability Kit, rabbit polyclonal antibodies to poly (ADP-ribose) polymerase (PARP) (#9542), extracellular signal-regulated kinase

1/2 (ERK1/2), phospho-ERK1/2 (Thr202/Tyr204), c-Jun N-terminal kinase 1/2 (JNK1/2), phospho-JNK1/2 (Thr183/Tyr185), p38, and phospho-p38 (Thr180/Tyr182) (MAPK Family Antibody Sampler Kit, #9926), FoxO3a (#2497), phospho-FOXO3a (Ser294) (#5538), E-cadherin (24E10) (#3195), β-catenin (D13A1) (#8814), and SignalFire Elite ECL Reagent (#12757) were from Cell Signaling Technologies (Beverly, MA, USA). Secondary antibodies goat polyclonal anti-mouse IgG H&L (HRP) (ab79023) (1:40000) and goat polyclonal anti-rabbit IgG H&L (HRP) (ab6721) (1:80000) were purchased from Abcam. The mitogen-activated protein kinase kinase (MEK) inhibitor PD0325901 was purchased from Selleckchem (Houston, TX, USA). The autophagic inhibitor 3-methyladenine (3-MA) was purchased from Selleckchem (Houston, TX, USA). All other chemicals were of the highest grade commercially available.

2.2 Cell culture

The human colon cancer SW620 cells (obtained from American Type Culture Collection (ATCC), Rockville, MD, USA), were grown in Dulbecco's modified Eagle's medium (DMEM) supplemented with 10% fetal bovine serum (FBS), 2 mM L-glutamine, penicillin 10 000 UI/mL and streptomycin 10 000 mg/mL (all from Lonza, Verviers, Belgium). The cells were grown routinely in tissue culture flasks (TPP, Trasadingen, Switzerland) at 37 °C in a 5% CO_2 humidified atmosphere.

2.3 Experimental design

Cells were treated with luteolin (1, 2, 5, and 10 μM) and medium only as a control. For studying autophagy, 5 mM 3-MA was used, and for studying MEK/ERK inhibition, 0.5 μM PD0325901 was used. Before treatments, cells were harvested and counted using Neubauer cell counting chamber (Roth, Karlsruhe, Germany) ($1x10^5$ cells/mL) and

grown in DMEM without antibiotics until 80–90% confluence in flasks and flat bottom 96-well chambers (TPP, Trasadingen, Switzerland). Cells were washed twice in phosphate-buffered saline (PBS), pH 7.4, and then exposed to DMEM containing a working concentration of each compound (the final concentrations of DMSO and Tween-80 in the medium were 0.005% and 0.1%, respectively) for 24 h before harvesting by trypsinization in 0.01% ethylenediaminetetraacetic acid (EDTA) (Lonza, Verviers, Belgium).

2.4 Colony formation assay

For the clonogenic assay, $1x10^5$ cells/mL were plated and treated with various doses of luteolin for 24 h. Then, for each treatment two hundred cells were counted (dead and alive), added to 6-well plates and cultured in medium containing 10% FBS until the number of cells per colony was ≥ 50 cells (7 d at 37 °C). After this, cells were fixed in ice-cold methanol for 20 min at 4 °C, stained with 0.5% crystal violet solution (methanol:water 25:75 (v/v)) (Merck, Germany) for 30 min and washed in PBS. Colonies were counted under a microscope (Olympus, Japan). *2.5 Cell viability assay*

The XTT (2,3-bis(2-methoxy-4-nitro-5-sulfophenyl)-2*H*-tetrazolium-5-carboxanilide) Cell Viability Kit (#9095, Cell Signaling Technologies (Beverly, MA, USA)) was used to determine the effect of different treatments on SW620 cell viability. Non-viable cells lose their metabolic capability to reduce the XTT into colored formazan dye. SW620 cells were treated and 24 h after, the absorbance was measured at 450 nm using a microplate reader (BioTek Elx808, Winooski, VT, USA).

2.5 Western blot

For immunoblot analysis, cells were harvested in 100 µL of RIPA lysis buffer containing 50 mM Tris-HCl pH 7.4, 150 mM NaCl, 1% NP-40, 0.5% sodium

deoxycholate, and 0.1% SDS, with the addition of 2 mM phenylmethyl sulphonyl fluoride, 1 mM sodium orthovanadate, and 2 μg/mL of each aprotinin, leupeptin, and pepstatin, for 1 h on ice. The protein concentration in samples was determined by the bicinchoninic acid (BCA) (Thermo Scientific Pierce, Rockford, IL, USA) method (Smith et al., 1985). To determine the target proteins, 30 or 60 μg protein/lane were loaded. Proteins were separated by 12.5%, 8%, or gradient SDS-polyacrylamide gel electrophoresis (SDS-PAGE) and transferred onto PVDF membrane. The membranes were blocked with 5% non-fat milk in Tris-buffered saline (TBS) with Tween-20 (1:10 v/v) for 2 h at room temperature and incubated with the primary antibodies against ERK1/2 (1:1000), phospho-ERK1/2 (1:2000), JNK1/2/3, p-JNK1/2, p38, phospho-p38, FOXO3a (1:1000), phospho-FOXO3a (1:1000), p21 (1:1000), Bax (1:3000), Bcl-2 (1:100), caspase-3 p11 (1:500), Atg7 (1:1000), Beclin-1 (1:500), Wnt3 (1:1000), E-cadherin (1:1000), β-catenin (1:1000), HO-1 (1:2000), SOD2 (1:4000), PARP (1:1000), and LC3B-I/II (1:1000) for 1 h at room temperature. The membranes were washed in TBS-Tween and incubated for 1 h with the secondary antibodies. After washing, chemiluminescent signals were detected using SignalFire Elite ECL Reagent and scanned (Allianze 4.0 Cambridge, UK). The intensity of the bands was assayed by computer image analysis ImageJ software (NIH, Bethesda, MD, USA).

2.6 Propidium iodide and acridine orange double staining

Apoptosis and necrosis induced by luteolin were analyzed using propidium iodide and acridine orange double staining described by Mascotti et al. (2000) and examined under a fluorescence microscope (Olympus BX51, Tokyo, Japan). SW620 were seeded at a concentration of 1×10^5 cells/mL and treated with different doses of luteolin. The cells were incubated in a 5% CO_2 atmosphere at 37 °C for 24 h. Cells were harvested,

centrifuged at low speed for 5 min, and washed twice using PBS. Pellet was resuspended in 10 µL of PBS containing AO (1 µg/mL) and PI (0.6 µg/mL). The freshly stained cell suspension was dropped onto a glass slide and observed under a fluorescence microscope within 5 min. AO and PI are intercalating nucleic acid-specific fluorochromes. AO enters all cells, both dead and alive and emits green fluorescence. Only AO in this staining can cross the plasma membrane of viable and early apoptotic cells. PI generates red fluorescence when present in dead cells and cells with compromised membranes. The criteria for identification were as follows: (a) viable cells have a green nucleus with an intact structure; (b) early apoptotic cells exhibit a bright-green nucleus showing condensation of chromatin in the nucleus; (c) late apoptotic cells show dense orange areas of chromatin condensation; (d) secondary necrotic cells have a red intact nucleus.

2.7 Acridine orange staining

The volume of the cellular acidic vacuoles, as a marker of autophagy, was visualized by AO staining (Paglin et al., 2001). After treatment with luteolin, cells were harvested and stained with 1 µg/mL AO in PBS. The cytoplasm and nucleus of the stained cells fluoresced bright green, whereas the acidic autophagic vacuoles fluoresced bright red. Fluorescent micrographs were taken using a fluorescence microscope (Olympus BX51, Tokyo, Japan).

2.8 TUNEL assay

Detection of apoptosis was performed using a commercially available terminal deoxynucleotidyl transferase dUTP nick end labeling (TUNEL) kit (Roche Diagnostics, Penzberg, Germany). Before treatments, $1x10^5$ cells/mL were seeded and grown until 80-90% confluence. After treatment with different doses of luteolin, as already

described, cells were fixed in ice-cold methanol for 15 min at -20 °C and incubated with blocking solution (3% H_2O_2 in methanol) for 10 min and incubated with TUNEL reaction mixture for 60 min at 37 ºC in a humidified chamber in the dark. The slides were stained with the nuclear stain DAPI and covered with an antifade medium (Mowiol 4-88). The immunofluorescence was analyzed by fluorescence microscopy using an Olympus BX51 microscope equipped by an Olympus DP 71 CCD digital camera.

2.9 Statistical analysis

Data were analyzed using StatSoft STATISTICA computer software (StatSoft Inc., Tulsa, USA). A comparison of mean values between groups was performed by the t-test and one-way ANOVA. Each experiment was repeated three times. Values in the text are means ± standard deviation (SD). Differences with $P < 0.05$ were considered statistically significant.

3 Results

3.1 Luteolin reduces the viability of SW620 cells

In order to evaluate the effect of luteolin on proliferation and the cytotoxic effect on colon cancer SW620 cells, we treated cells with various concentrations of luteolin followed by the viability and colony-forming assays. Fig. 1A shows the effect of luteolin on SW620 cell's viability after 24 h exposure. The viability of colon cancer cells was dose-dependently inhibited by luteolin, with the IC_{50} (50% inhibitory concentration) 48.8 ± 1.6 μM. At lower concentrations, luteolin showed dose-dependent apoptotic cell death, causing necrosis only at higher concentrations (≥ 20 μM) (Fig. 2). Therefore, we choose luteolin at a concentration ≤ 10 μM for further experiments.

Colony formation assay results showed that luteolin significantly decreased the colony number in a dose-dependent manner compared to control cells (Fig. 1B).

3.2 Luteolin induces oxidative stress in SW620 cells

To determine the effect of luteolin on the antioxidant status in SW620 cells we analyzed the expression of antioxidant enzymes HO-1 and SOD2 (Fig. 3A). Incubation of SW620 cells with luteolin dose-dependently increased HO-1 and SOD2 expression compared to control cells (Fig. 3B and C). Our results indicated that luteolin modulated the redox status of the cells by upregulating the level of antioxidant enzymes.

3.3 Luteolin induces SW620 cells apoptosis

To clarify the mechanism underlying the inhibitory effect of luteolin on SW620 cell viability, apoptosis was determined by western blot analysis of apoptosis-related protein expression and TUNEL assay. Treatment with luteolin resulted in dose-dependent apoptotic cell death in the cancer cells (Fig. 4A). Luteolin dose-dependently decreased Bcl-2 expression (Fig. 4B) and increased expression of Bax (Fig. 4C). A concomitant increase in caspase-3 (Fig. 4E) and PARP (Fig. 4F) cleavage indicated increased apoptotic cell death by luteolin. The TUNEL assay confirmed the results of apoptosis analysis by western blot, showing an increased number of TUNEL-positive cells by increasing luteolin concentration (Fig. 5). Levels of p21, an inhibitor of the cell cycle, were also increased by luteolin treatment (Fig. 4D).

3.4 Luteolin induces SW620 cells autophagy

To evaluate the effect of luteolin on autophagy in SW620 cells, we measured the expression of autophagy-related proteins involved in the formation of autophagosomes, Atg7, Beclin-1, and LC3B-I/II (Fig. 6A). Treatment with luteolin increased the expression of both LC3B-I and LC3B-II in a dose-dependent manner (Fig. 6B).

Similarly, Atg7 and Beclin-1 expression in SW620 cell lysates increased after luteolin treatment (Fig. 6C and D). Acridine orange staining showed increased formation of autophagic vacuoles by treatment with luteolin (Fig.7).

3.5 Luteolin increases MAPK expression in SW620 cells

To determine the effect of luteolin on the MAPK signaling pathway, we investigated the expression of ERK1/2, JNK1/2, and p38 (Fig. 8A). Treatment with luteolin increased expression of phospho-ERK1/2 in a dose-dependent manner, indicating activation of ERK1/2 (Fig. 8B). Similarly, phospho-JNK1/2 and phospho-p38 expression (Fig. 8C and D) was dose-dependently increased by luteolin, indicating that SW620 cytotoxic activity of luteolin was associated with activation of the ERK, JNK, and p38 pathways.

3.6 Luteolin increases FOXO3a expression in SW620 cells

In order to further clarify the mechanism of luteolin cytotoxicity in SW610 cells, we determined the activation of FOXO3a pathway. Our results showed that luteolin dose-dependently increased FOXO3a expression (Fig. 8E). The expression level of phospho-FOXO3a, which was also induced by luteolin, was lower than that of FOXO3a (Fig. 8E).

3.7 Autophagy inhibition sensitizes luteolin treated SW620 cells to apoptosis

Fig. 9A shows the effect of the autophagy inhibitor, 3-MA, on SW620 cells viability. Treatment with 3-MA resulted in reduced viability of luteolin-treated SW620 cells, suggesting the cytoprotective role of autophagy induced by luteolin.

3.8. Inhibition of MEK/ERK signaling induces apoptosis in SW620 cells

Treatment with the MEK inhibitor PD0325901, as expected, inhibited phosphorylation of ERK and ERK-dependent FOXO3a phosphorylation (Fig. 9B), resulting in increased PARP cleavage and suppression of LC3B-I/II expression in SW620 cells. MEK/ERK

inhibition also reduced the viability of SW620 cells and potentiated the cytotoxicity of luteolin (Fig. 9C).

3.9. Luteolin reverses EMT in SW620 cells

To examine the antimetastatic effect of luteolin in SW620 cells, the expression of proteins involved in the EMT process was measured (Fig. 10). Treatment with luteolin reduced the expression of Wnt3 and β-catenin in a dose-dependent manner, with concomitant induction of E-cadherin.

4 Discussion

The results of the current study show that luteolin 1) induces oxidative stress, 2) reduces cell viability and proliferation and induces apoptotic cell death, 3) induces cytoprotective autophagy, and 4) reverses EMT in metastatic colon cancer SW620 cell line. Reactive oxygen species (ROS) play a key role in both cancer development and therapy. Cancer cells demand high ROS concentrations to maintain their high proliferation rate (Sosa et al., 2013). The activation of the antioxidant Nrf2/HO-1 pathway by phytochemicals has been shown as a critical step in colon cancer chemoprevention (Bi et al., 2018). The apoptotic and anticancer effects of luteolin were also associated with HO-1 induction and increased antioxidant defense in HT-29 and SNU-407 colon cancer cells (Kang et al., 2019). Among the antioxidant enzymes, only SOD2 is located within the mitochondria, a major site for ROS production. A previous study showed that the anticancer effect of natural compound columbianadin in HCT-116 colon cancer cells was associated with the increase in expression of mitochondrial SOD2 enzyme (Kang, Hong, Choi, & Lee, 2016). In the current study, increased expression of HO-1 and SOD2 suggested the induction of oxidative stress by luteolin, which coincided with apoptotic cell death in SW620 colon cancer cells .

The cytotoxicity of luteolin in the current study coincided with increased phosphorylation of MAPKs. The role of MAPKs in cancer is as pleiotropic as cancer itself (Dhillon et al., 2007). The ERK signaling pathway plays a key role in several steps of cancer development (Samatar & Poulikakos, 2014). This pathway is often upregulated in human tumors, promoting the survival of cancer cells by regulating the levels and activities of proapoptotic proteins (Kohno & Pouyssegur, 2006). Stress-activated JNK or p38 pathways can induce apoptosis in some cases but lead to increased survival in others or even exhibit antagonistic effects on cell proliferation and survival (Wagner & Nebreda, 2009). In the current study, luteolin-induced activations of ERK1/2, JNK1/2, and p38 in SW620 cells coincided with increased apoptosis, evidenced by the increase in caspase-3 and PARP cleavage and TUNEL positivity, as well as the reduced cell viability and proliferation. Recently, Kang et al. (2017) showed the induction of apoptosis in HT-29 colon cancer cells by luteolin through JNK and p38 but not ERK-dependent pathway. However, another study showed that induction of ERK by natural compounds in colon cancer cells could be antiapoptotic and tumorigenic (Chen, Jin, & Xu, 2016). Indeed, the MEK/ERK inhibition resulted in apoptosis and reduced proliferation in several cancer cell lines (Liu et al., 2016; Meng et al., 2010). Our current results support these findings, showing that blocking ERK activation by PD0325901 potentiate the proapoptotic activity of luteolin evidenced by increased PARP cleavage.

The ERK pathway is involved in the regulation of FOXO3a, a ubiquitously expressed transcription factor that plays an important role in carcinogenesis (Eijkelenboom & Burgering, 2013). The phosphorylation of FOXO3a by ERK leads to its nuclear exclusion and the loss of transcriptional activity. Increased FOXO3a

expression in cancer cells is associated with oxidative detoxification, cell cycle arrest, inhibition of proliferation, and apoptosis, while its inactivation has been associated with the initiation and progression of cancer (Liu et al., 2018; Taylor et al., 2015). Moreover, the regulation of the FOXO3a activity has been suggested as a molecular link between apoptosis and autophagy (Fitzwalter et al., 2018). Previously, luteolin has been shown to exhibit antiproliferative and apoptotic effects against breast cancer cells by inducing FOXO3a expression and elevating the expression of FOXO3a targets p21 and p27 (Lin et al., 2015). In the current study, the apoptotic activity of luteolin was associated with increased expression of FOXO3a and its targets, p21 and SOD2. Luteolin also increased ERK-mediated FOXO3a phosphorylation on Ser294, however, this increase was overshadowed by strong FOXO3a expression, suggesting an additional, ERK-independent mechanism of FOXO3a induction, as the result of the shift in the balance of prosurvival and proapoptotic signaling toward antiproliferative mechanisms (Sharma et al., 2006). In support of the phenomenon of "oncogene addiction" suggested by Sharma and coworkers, the inhibition of MEK/ERK in the current study resulted in increased FOXO3a expression, which was associated with increased apoptosis and cytotoxicity by luteolin.

Autophagy is a well-known molecular mechanism of selective degradation of damaged cellular proteins and other components (Cheng, 2019). Several signaling pathways are involved in the regulation of autophagy, including ERK (Martinez-Lopez, Athonvarangkul, Mishall, Sahu, & Singh, 2013) and JNK and p38 (Sui et al., 2014). Autophagy can play a prodeath or prosurvival role depending on the cell type and the type of specific stimuli, the stage of progression, as well as the intensity of Beclin-1 induction (Amaravadi, Kimmelman, & White, 2016; Sui et al., 2014). In the current

study, luteolin increased expression of Atg7, Beclin-1, and LC3B-II and increased the formation of acidic autophagic vacuoles in SW620 cells, suggesting that luteolin acted not only as an inducer of apoptosis but also autophagy. The inhibition of autophagy by 3-MA suggested that autophagy was activated as a compensatory mechanism to resist luteolin-mediated apoptosis. Similarly, Liu et al. (2017) showed that inhibition of autophagy leads to reduced cancer cell proliferation and activation of apoptosis in SW620 cells. Luteolin has been shown to induce cytoprotective autophagy in several cancer cell lines (Lee & Kwon, 2019; Chakrabarti & Ray, 2016; Verschooten et al., 2012). The non-canonical MEK/ERK signaling pathway has been involved in the regulation of autophagy in cancer cells (Wang et al., 2009). The depletion of ERK partially inhibited autophagy, whereas specific inhibition of MEK completely inhibited it (Wang et al., 2009). In the current study, the inhibition of cytoprotective autophagy through the suppression of LC3B-II formation by MEK/ERK inhibition contributed to the cytotoxicity of luteolin in SW620 cells.

FOXO proteins were suggested as activators of autophagy through direct transactivation of autophagy genes or by regulating autophagy activity (Cheng, 2019). However, FOXO3a was shown as a negative regulator of autophagy in multiple cancer cell lines, including prostate, breast, and colon cancer, suggesting a complexity of FOXO signaling in different cell contexts (Zhu et al., 2014). Our results support these findings, showing that increased FOXO3a expression following the ERK inhibition coincided with reduced LC3B-II expression, suggesting the suppression of autophagy through the ERK/FOXO3a signaling.

Epithelial-mesenchymal transition (EMT) is an early event in tumor metastasis. It allows a polarized epithelial cell to acquire a mesenchymal cell phenotype, which

includes enhanced migratory capacity, invasiveness, elevated resistance to apoptosis and increased production of the extracellular matrix proteins (Kalluri and Weinberg, 2009). Therefore, targeting the EMT pathways represents an attractive strategy for cancer treatment (Mittal, 2018). Several studies suggested that the Wnt/β-catenin pathway plays a key role in EMT (Pai et al., 2017; Duchartre et al., 2016). Our results showed the ability of luteolin to reverse the EMT process through a mechanism that involves the suppression of the Wnt/β-catenin pathway, suggesting its antimetastatic potential in SW620 cells. The previous report suggested the protective effect of luteolin in azoxymethane-induced colon cancer via inhibition of the Wnt/β-catenin pathway (Ashokkumar & Sudhandiran, 2011). It has been also suggested that FOXO3a inhibits malignant phenotypes that are dependent on β-catenin transcriptional activity and modulation of EMT (Liu et al., 2015), which is consistent with our results. In conclusion, luteolin exhibited the cytotoxicity against metastatic colon cancer SW620 cells through activation of apoptosis via ERK1/2 and FOXO3a-dependent pathways, with concomitant induction of the cytoprotective autophagy. Luteolin also showed the antimetastatic potential through the suppression of the Wnt/β-catenin pathway. These results suggest the luteolin could be considered as an anticancer agent for the treatment of advanced stages of colon cancer in humans, although further clinical studies should be performed to confirm these findings.

Acknowledgments

This research was supported by grants from the University of Rijeka (Projects 13.06.1.2.24 and 13.06.2.2.60).

Conflict of interest

We confirm that there are no known conflicts of interest associated with this publication.

References

Amaravadi, R., Kimmelman, A. C., & White, E. (2016). Recent insights into the function of autophagy in cancer. *Genes and Development, 30(17),* 1913-1930.

Ashokkumar, P., & Sudhandiran, G. (2011). Luteolin inhibits cell proliferation during Azoxymethane-induced experimental colon carcinogenesis via Wnt/β-catenin pathway. *Investigational New Drugs, 29*(2), 273-284.

Bi, W., He, C. N., Li, X. X., Zhou, L. Y., Liu, R. J., Zhang, S., . . . Zhang, P. F. (2018). Ginnalin A from Kujin tea (*Acer tataricum* subsp. *ginnala*) exhibits a colorectal cancer chemoprevention effect via activation of the Nrf2/HO-1 signaling pathway. *Food and Function, 9*(5), 2809-2819. Brandt R., Sell, T., Lüthen, M., Uhlitz, F., Klinger, B,, Riemer, P., . . . Morkel, M. (2019). Cell type-dependent differential activation of ERK by oncogenic KRAS in colon cancer and intestinal epithelium. *Nature Communications, 10*(1), 2919.

Burotto, M., Chiou, V. L., Lee, J. M., & Kohn, E. C. (2014). The MAPK pathway across different malignancies: a new perspective. *Cancer, 120*(22), 3446-3456.

Chakrabarti, M., & Ray, S. K. (2016). Anti-tumor activities of luteolin and silibinin in glioblastoma cells: overexpression of miR-7-1-3p augmented luteolin and silibinin to inhibit autophagy and induce apoptosis in glioblastoma *in vivo*. *Apoptosis, 21(3),* 312-328.

Chen, H., Jin, Z. L., & Xu, H. (2016). MEK/ERK signaling pathway in apoptosis of SW620 cell line and inhibition effect of resveratrol. *Asian Pacific Journal of Tropical Medicine, 9*(1), 49-53.

Cheng, Z. (2019). The FoxO-autophagy axis in health and disease. *Trends in Endocrinology & Metabolism, 30(9),* 658-671.

Coomans de Brachène, A., & Demoulin, J. B. (2016). FOXO transcription factors in cancer development and therapy. *Cellular and Molecular Life Sciences, 73*(6), 1159-1172.

Dhillon, A. S., Hagan, S., Rath, O., & Kolch, W. (2007). MAP kinase signalling pathways in cancer. *Oncogene, 26(22),* 3279-3290.

Domitrovic, R., Cvijanovic, O., Pugel, E. P., Zagorac, G. B., Mahmutefendic, H., & Skoda, M. (2013). Luteolin ameliorates cisplatin-induced nephrotoxicity in mice through inhibition of platinum accumulation, inflammation and apoptosis in the kidney. *Toxicology, 310*, 115-123.

Domitrovic, R., Jakovac, H., Tomac, J., & Sain, I. (2009). Liver fibrosis in mice induced by carbon tetrachloride and its reversion by luteolin. *Toxicology and Applied Pharmacology, 241*(3), 311-321.

Duchartre, Y., Kim, Y. M., & Kahn, M. (2016). The Wnt signaling pathway in cancer. *Critical Reviews in Oncology Hematology, 99*, 141-149.

Eijkelenboom, A., & Burgering, B. M. (2013). FOXOs: signalling integrators for homeostasis maintenance. *Nature Reviews Molecular Cell Biology, 14*(2), 83-97.

Fernández de Mattos, S., Villalonga, P., Clardy, J., & Lam, E. W. (2008). FOXO3a mediates the cytotoxic effects of cisplatin in colon cancer cells. *Molecular Cancer Therapeutics, 7*(10), 3237-3246.

Fitzwalter, B. E., Towers, C. G., Sullivan, K. D., Andrysik, Z., Hoh, M., Ludwig, M., . . . Thorburn, A. (2018). Autophagy inhibition mediates apoptosis sensitization in cancer therapy by relieving FOXO3a turnover. *Developmental Cell, 44*(5), 555-565.

Hewitt, R. E., McMarlin, A., Kleiner, D., Wersto, R., Martin, P., Tsokos, M., . . . Stetler-Stevenson, W. G. (2000). Validation of a model of colon cancer progression. *The Journal of Pathology, 192*(4), 446-454.

Imran, M., Rauf, A., Abu-Izneid, T., Nadeem M., Shariati, M. A., Khan, I. A., . . . Mubarak, M. S. (2019). Luteolin, a flavonoid, as an anticancer agent: A review. *Biomedicine & Pharmacotherapy, 112*, 108612.

Juan, T. K., Liu, K. C., Kuo, C. L., Yang, M. D., Chu, Y. L., Yang, J. L., . . . Chung, J. G. (2018). Tetrandrine suppresses adhesion, migration and invasion of human colon cancer SW620 cells via inhibition of nuclear factor-kappaB, matrix metalloproteinase-2 and matrix metalloproteinase-9 signaling pathways. *Oncology Letters, 15*(5), 7716-7724.

Kalluri, R., & Weinberg, R. A. (2009). The basics of epithelial-mesenchymal transition. *Journal of Clinical Investigation, 119*(6), 1420-1428.

Kang, J. I., Hong, J. Y., Choi, J. S., & Lee, S. K. (2016). Columbianadin inhibits cell proliferation by inducing apoptosis and necroptosis in HCT116 colon cancer cells. *Biomolecules and Therapeutics (Seoul), 24*(3), 320-327.

Kang, K. A., Piao, M. J., Hyun, Y. J., Zhen, A. X., Cho, S. J., . . . Hyun, J. W. (2019). Luteolin promotes apoptotic cell death via upregulation of Nrf2 expression by DNA demethylase and the interaction of Nrf2 with p53 in human colon cancer cells. *Experimental & Molecular Medicine, 51*(4), 1-14.

Kang, K. A., Piao, M. J., Ryu, Y. S., Hyun, Y. J., Park, J. E., Shilnikova, K., . . . Hyun, J. W. (2017). Luteolin induces apoptotic cell death via antioxidant activity in human colon cancer cells. *International Journal of Oncology, 51*(4), 1169-1178.

Kohno, M., & Pouyssegur, J. (2006). Targeting the ERK signaling pathway in cancer therapy. *Annals of Medicine, 38*(3), 200-211.

Kustiawan, P. M., Lirdprapamongkol, K., Palaga, T., Puthong, S., Phuwapraisirisan, P., Svasti, J., & Chanchao, C. (2017). Molecular mechanism of cardol, isolated from *Trigona incisa* stingless bee propolis, induced apoptosis in the SW620 human colorectal cancer cell line. *BMC Pharmacology and Toxicology, 18*(1), 32.

Lee, Y., & Kwon, Y. H. (2019). Regulation of apoptosis and autophagy by luteolin in human hepatocellular cancer Hep3B cells. *Biochemical and Biophysical Research Communications, 517(4)*, 617-622.

Lin, C. H., Chang, C. Y., Lee, K. R., Lin, H. J., Chen, T. H., & Wan, L. (2015). Flavones inhibit breast cancer proliferation through the Akt/FOXO3a signaling pathway. *BMC Cancer, 15*.

Liu, H., Yin, J., Wang, H., Jiang, G., Deng, M., Zhang, G., . . . He, Z. (2015). FOXO3a modulates WNT/β-catenin signaling and suppresses epithelial-to-mesenchymal transition in prostate cancer cells. *Cellular Signaling, 27*(3), 510-518.

Liu, J., Ma, L. N., Chen, X., Wang, J. X., Yu, T., Gong, Y., . . . Liang, H. (2016). ERK inhibition sensitizes cancer cells to oleanolic acid-induced apoptosis through ERK/Nrf2/ROS pathway. *Tumor Biology, 37*(6), 8181-8187.

Liu, L., Zhao, W. M., Yang, X. H., Sun, Z. Q., Jin, H. Z., Lei, C., . . . Wang, H. J. (2017). Effect of inhibiting Beclin-1 expression on autophagy, proliferation and apoptosis in colorectal cancer. *Oncology Letters, 14*(4), 4319-4324.

Liu, Y., Ao, X., Ding, W., Ponnusamy, M., Wu, W., Hao, X., . . . Wang, J. (2018). Critical role of FOXO3a in carcinogenesis. *Molecular Cancer, 17*(1), 104.

Martinez-Lopez, N., Athonvarangkul, D., Mishall, P., Sahu, S., & Singh, R. (2013). Autophagy proteins regulate ERK phosphorylation. *Nat Commun, 4*, 2799.

Mascotti, K., McCullough, J., & Burger, S. R. (2000). HPC viability measurement: trypan blue versus acridine orange and propidium iodide. *Transfusion, 40*(6), 693-696.

Meng, J. R., Fang, B. L., Liao, Y., Chresta, C. M., Smith, P. D., & Roth, J. A. (2010). Apoptosis induction by MEK Inhibition in human lung cancer cells is mediated by Bim. *Plos One, 5*(9).

Mittal, V. (2018). Epithelial mesenchymal transition in tumor metastasis. *Annual Review of Pathology: Mechanisms of Disease 13*, 395-412.

Newman, D. J., & Cragg, G. M. (2016). Natural products as sources of new drugs from 1981 to 2014. *Journal of Natural Products, 79*(3), 629-661.

Paglin, S., Hollister, T., Delohery, T., Hackett, N., McMahill, M., Sphicas, E., . . . Yahalom, J. (2001). A novel response of cancer cells to radiation involves autophagy and formation of acidic vesicles. *Cancer Research, 61*(2), 439-444.

Pai, S. G., Carneiro, B. A., Mota, J. M., Costa, R., Leite, C. A., Barroso-Sousa, R., . . . Giles, F. J. (2017). Wnt/beta-catenin pathway: modulating anticancer immune response. *Journal of Hematology & Oncology, 10*.

Redondo-Blanco, S., Fernandez, J., Gutierrez-Del-Rio, I., Villar, C. J., & Lombo, F. (2017). New insights toward colorectal cancer chemotherapy using natural bioactive compounds. *Frontiers in Pharmacology, 8*, 109.

Samatar, A. A., & Poulikakos, P. I. (2014). Targeting RAS-ERK signalling in cancer: promises and challenges. *Nature Reviews Drug Discovery, 13*(12), 928.

Seelinger, G., Merfort, I., & Schempp, C. M. (2008). Anti-oxidant, anti-inflammatory and anti-allergic activities of luteolin. *Planta Medica, 74*(14), 1667-1677.

Sharma, S. V., Gajowniczek, P., Way, I. P., Lee, D. Y., Jiang, J., Yuza, Y., . . . Settleman, J. (2006). A common signaling cascade may underlie "addiction" to the Src, BCR-ABL, and EGF receptor oncogenes. *Cancer Cell, 10*(5), 425-435.

Shimoi, K., Okada, H., Furugori, M., Goda, T., Takase, S., Suzuki, M., . . . Kinae, N. (1998). Intestinal absorption of luteolin and luteolin 7-O-beta-glucoside in rats and humans. *FEBS Letters, 438*(3), 220-224.

Siegel, R. L., Miller, K. D., Fedewa, S. A., Ahnen, D. J., Meester, R. G. S., Barzi, A., & Jemal, A. (2017). Colorectal cancer statistics, 2017. *CA Cancer Journal for Clinicians, 67*(3), 177-193.

Smith, P. K., Krohn, R. I., Hermanson, G. T., Mallia, A. K., Gartner, F. H., Provenzano, M. D., . . . Klenk, D. C. (1985). Measurement of protein using bicinchoninic acid. *Analytical Biochemistry, 150*(1), 76-85.

Sui, X., Kong, N., Ye, L., Han, W., Zhou, J., Zhang, Q., . . . Pan, H. (2014). p38 and JNK MAPK pathways control the balance of apoptosis and autophagy in response to chemotherapeutic agents. *Cancer Letters, 344*(2), 174-179.

Taylor, S., Lam, M., Pararasa, C., Brown, J. E. P., Carmichael, A. R., & Griffiths, H. R. (2015). Evaluating the evidence for targeting FOXO3a in breast cancer: a systematic review. *Cancer Cell International, 15(1),* 1.

Tuorkey, M. J. (2016). Molecular targets of luteolin in cancer. *European Journal of Cancer Prevention, 25*(1), 65-76.

Verschooten, L., Barrette, K., Van Kelst, S., Rubio Romero, N., Proby, C., De Vos, R., . . . Garmyn, M. (2012). Autophagy inhibitor chloroquine enhanced the cell death inducing effect of the flavonoid luteolin in metastatic squamous cell carcinoma cells. *PLOS One, 7*(10), e48264.

Wagner, E. F., & Nebreda, A. R. (2009). Signal integration by JNK and p38 MAPK pathways in cancer development. *Nature Reviews Cancer, 9*(8), 537-549.

Wang, J. R., Whiteman, M. W., Lian, H. Q., Wang, G. X., Singh, A., Huang, D. Y., & Denmark, T. (2009). A non-canonical MEK/ERK signaling pathway regulates autophagy via regulating Beclin 1. *Journal of Biological Chemistry, 284*(32), 21412-21424.

You, Y. J., Wang, R., Shao, N. Y., Zhi, F., & Yang, Y. L. (2019). Luteolin suppresses tumor proliferation through inducing apoptosis and autophagy via MAPK activation in glioma. *Oncotargets and Therapy, 12*, 2383-2395.

Zhao, W. H., Shi, F. Q., Guo, Z. K., Zhao, J. L., Song, X. Y., & Yang, H. (2018). Metabolite of ellagitannins, urolithin A induces autophagy and inhibits metastasis in human sw620 colorectal cancer cells. *Molecular Carcinogenesis, 57*(2), 193-200.

Zhu, W. L., Tong, H., Teh, J. T., & Wang, M. (2014). Forkhead box protein O3 transcription factor negatively regulates autophagy in human cancer cells by inhibiting forkhead box protein O1 expression and cytosolic accumulation. *PLoS One, 9(12),* e115087.

Figure captions:

Fig. 1. Dose-dependent effect of luteolin on SW620 cell proliferation and viability. For XTT viability assay the cells were cultured in 10% FBS medium and treated with luteolin for 24 h (A). The percent cytotoxicity was calculated in comparison to untreated cells taken as 100%. The 50% inhibitory concentration (IC_{50}) was determined using the non-linear regression analysis. The proliferation capacity of SW620 cells was determined by colony formation assay 24 h after treatment with various doses of luteolin (B). The number of colony formation was counted under the microscope. The number of cells per colony was ≥ 50 cells. Values are expressed as mean ± SD from three independent experiments.

Fig. 2. Representative acridine orange/propidium iodide microphotographs for detection of apoptosis and necrosis in SW620 control cells (A) and cells treated with luteolin at doses of 1 μM (B), 2 μM (C), 5 μM (D), 10 μM (E), and 20 μM (F). Treatment with higher doses of luteolin has resulted in an increased occurrence of apoptotic and necrotic cells. N, necrosis (red intact nucleus); EA, early apoptosis (bright-green nucleus showing condensation of chromatin in the nucleus); LA, late apoptosis (dense orange areas of chromatin condensation).

Fig. 3. Analysis of oxidative stress in SW620 cells treated with luteolin. Representative immunoblots of HO-1 and SOD2 expression (A). Treatment with luteolin resulted in increased expression of HO-1 (B), which was the highest by the lowest dose of luteolin. The increase in SOD2 expression was dose-dependent (C). Values are expressed as mean ± SD from three independent experiments. * $P < 0.05$ vs untreated cells.

Fig. 4. Analysis of apoptotic cell death in SW620 cells treated with luteolin. Representative immunoblots of Bax, Bcl-2, p21, caspase-3, and PARP expression (A). Treatment with luteolin resulted in a dose-dependent decrease in expression of Bcl-2 (B) with a concomitant increase of Bax (C) and p21 (D) expression, as well as increased cleavage of caspase-3 (E) and PARP (F). Values are expressed as mean ± SD from three independent experiments. $^{*,\#}P < 0.05$ vs untreated cells.

Fig. 5. Representative micrographs for detection of apoptotic cell death by the immunofluorescence TUNEL assay. Treatment of SW620 cells with luteolin at doses of 1 μM (B), 5 μM (C), and 10 μM (D) has resulted in a dose-dependent increase in the occurrence of TUNEL-positive cells compared to untreated cells (A).

Fig. 6. Analysis of autophagy in SW620 cells treated with luteolin. Representative immunoblots of LC3B, Atg7, and Beclin-1 expression (A). Treatment with luteolin resulted in increased expression of both LC3B-I and LC3B-II (B) as well as increased expression of Atg7 (C) and Beclin-1 (D). Values are expressed as mean ± SD from three independent experiments. $^{*,\#}P < 0.05$ vs untreated cells.

Fig. 7. Representative acridine orange micrographs for detection of autophagy by the immunofluorescence microscopy in control cells (A) and cells treated with luteolin at doses of 2 μM (B), 5 μM (C), and 10 μM (D). The cytoplasm and nucleus of the stained cells emit bright green fluorescence, whereas the acidic autophagic vacuoles emit bright red fluorescence. Treatment with higher doses of luteolin has resulted in an increased occurrence of autophagic vacuoles in the cell.

Fig. 8. Analysis of signaling pathways in SW620 cells treated with luteolin. Representative immunoblots of MAPK and FOXO3a expression (A). Administration of luteolin resulted in increased phosphorylation of ERK1/2 (Thr202/Tyr204) (B), JNK1/2 (Thr183/Tyr185) (C), and p38 (Thr180/Tyr182) (D), compared to their inactive forms. Luteolin also markedly increased FOXO3a expression (E), with a small increase in FOXO3a (Ser294) phosphorylation. Values are expressed as mean ± SD from three independent experiments. $^{*,\#}P < 0.05$ vs untreated cells.

Fig. 9. The effect of autophagy inhibition on luteolin cytotoxicity (A). The autophagy inhibitor 3-MA (5 mM) reduced viability of SW620 cells treated with luteolin compared to luteolin-only treated cells. Inhibition of MEK/ERK signaling in SW620 cells: representative immunoblots of ERK1/2, FOXO3a, phospho-FOXO3a (Ser294), PARP, and LC3B-I/II expression (B). Administration of the MEK inhibitor PD0325901 resulted in the inhibition of phosphorylation of ERK1/2 and FOXO3a, with a concomitant increase in FOXO3a and decrease in LC3B-I/II expression. The MEK/ERK inhibition was associated with reduced cell viability and increased cytotoxicity of luteolin (C). Values are expressed as mean ± SD from three independent experiments. ^{a,b} Different letters indicate a statistical difference between treatments ($P < 0.05$).

Fig. 10. Reversal of the EMT process in SW620 cells treated with luteolin. Representative immunoblots of Wnt3, β-catenin, and E-cadherin (A). Administration of luteolin resulted in reduced expression of Wnt3 (B) and β-catenin (C), with concomitant

induction of E-cadherin (D). Values are expressed as mean ± SD from three independent experiments. * $P < 0.05$ vs untreated cells.

Declaration of interests

☒ The authors declare that they have no known competing financial interests or personal relationships that could have appeared to influence the work reported in this paper.

☐The authors declare the following financial interests/personal relationships which may be considered as potential competing interests:

Graphical abstract

- Luteolin reduced the viability of SW620 cells and induced oxidative stress
- The expression of proapoptotic proteins increased by luteolin treatment
- Luteolin increased expression of autophagic proteins and a prosurvival autophagy
- Luteolin induces reversal of the epithelial-mesenchymal transition
- Luteolin activated the ERK1/2 and forkhead box O3a signaling pathways
- ERK inhibition increased FOXO3a expression and apoptosis and suppressed autophagy

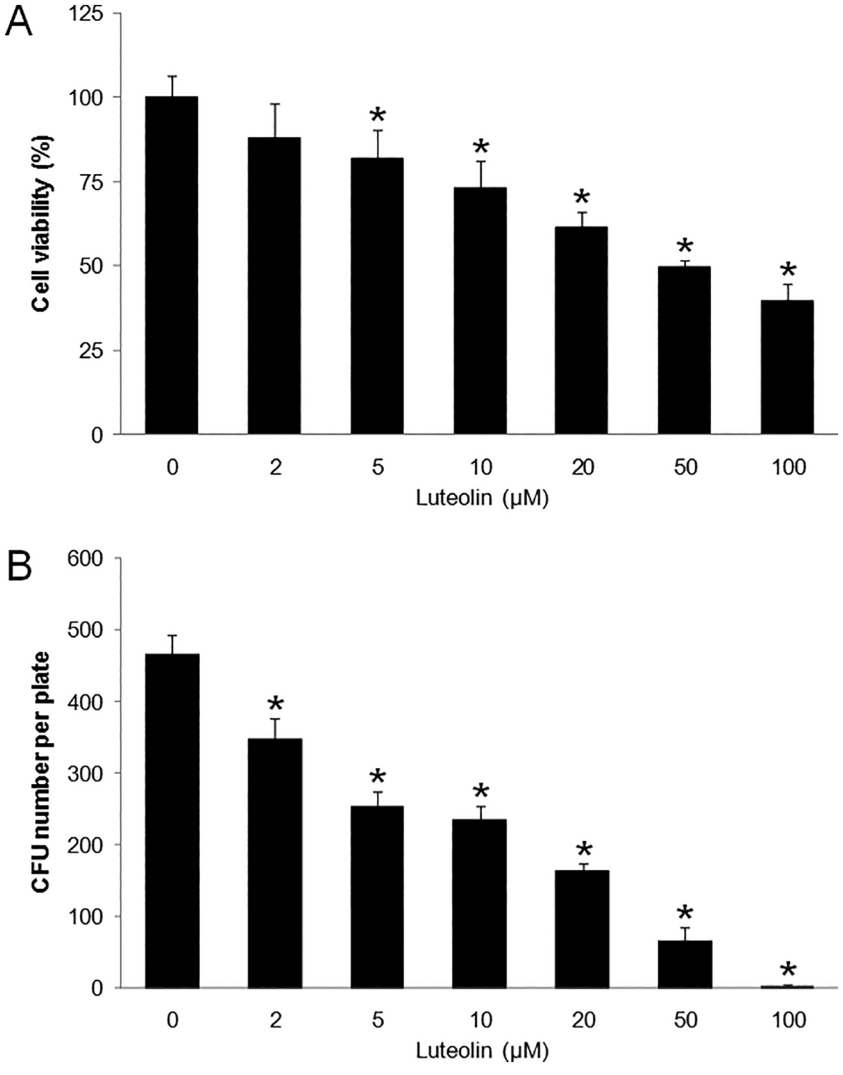
A
125
100
75
50
25
0
Cell viability (%)
*
0
2
5
10
20
50
100
Luteolin (μM)
B
600
500
400
300
200
100
0
CFU number per plate
*
0
2
5
10
20
50
100
Luteolin (μM)

Figure 1

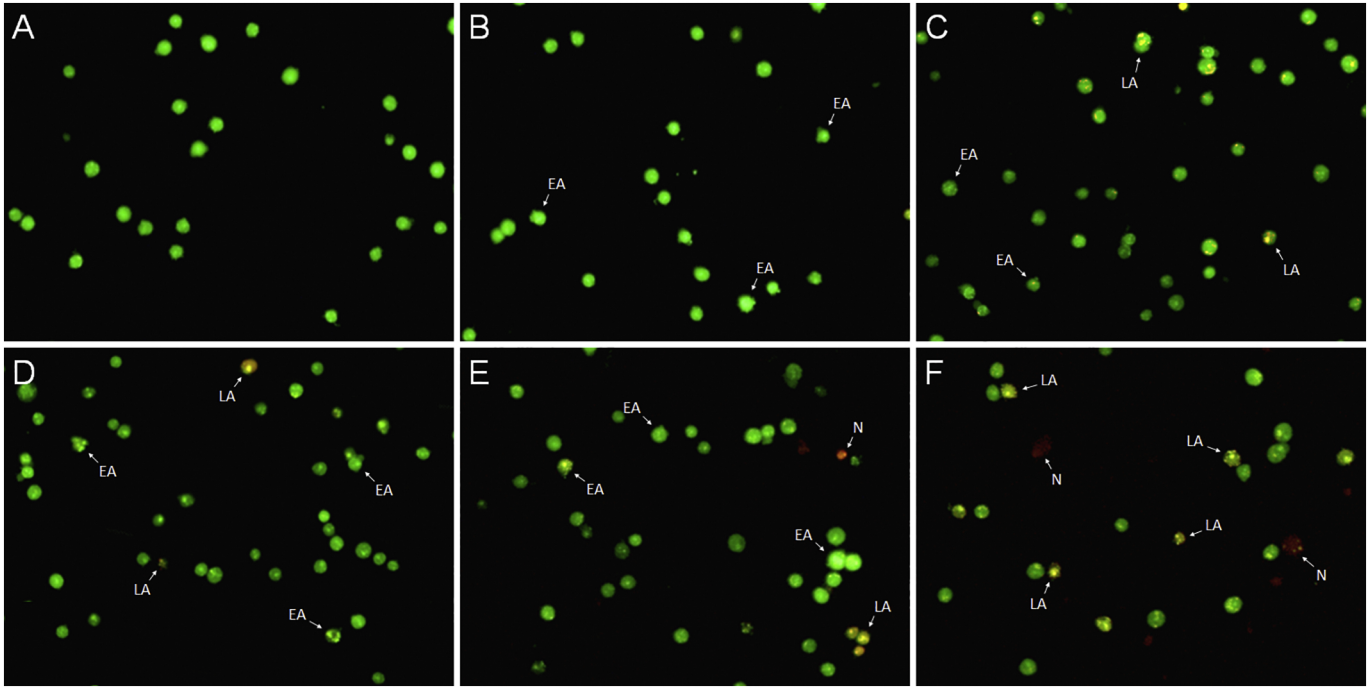

Figure 2

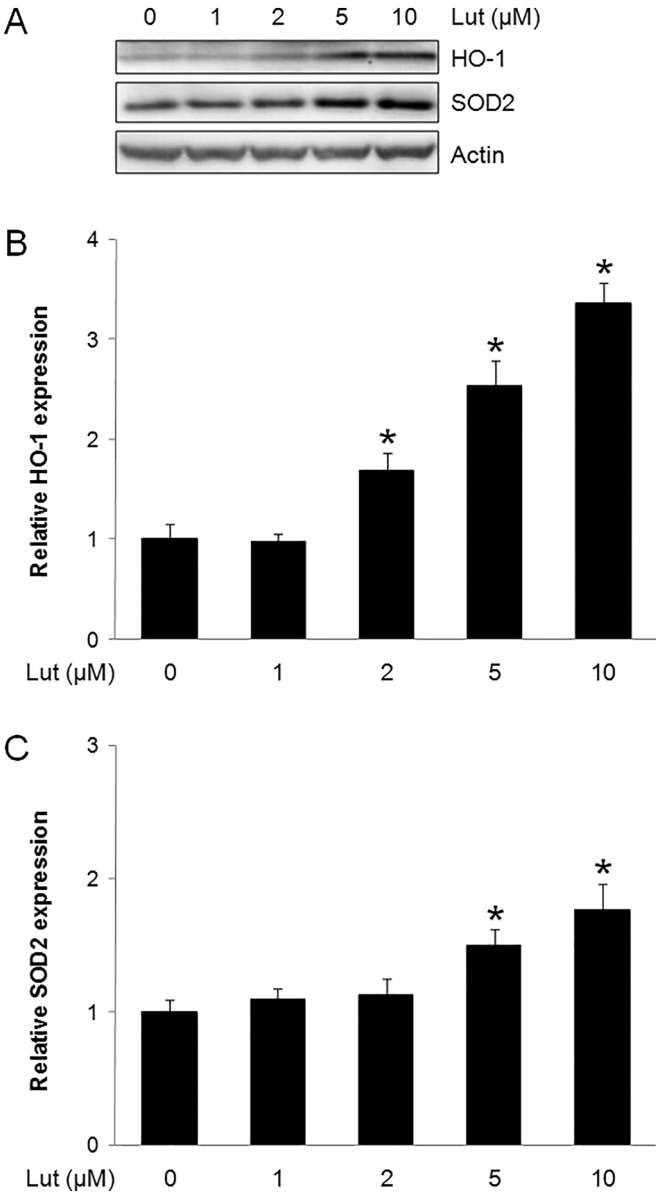
A
0
1
2
5
10
Lut (μM)
HO-1
SOD2
Actin
B
Relative HO-1 expression
4
3
2
1
0
*
*
*
Lut (μM)
0
1
2
5
10
C
Relative SOD2 expression
3
2
1
0
*
*
Lut (μM)
0
1
2
5
10

Figure 3

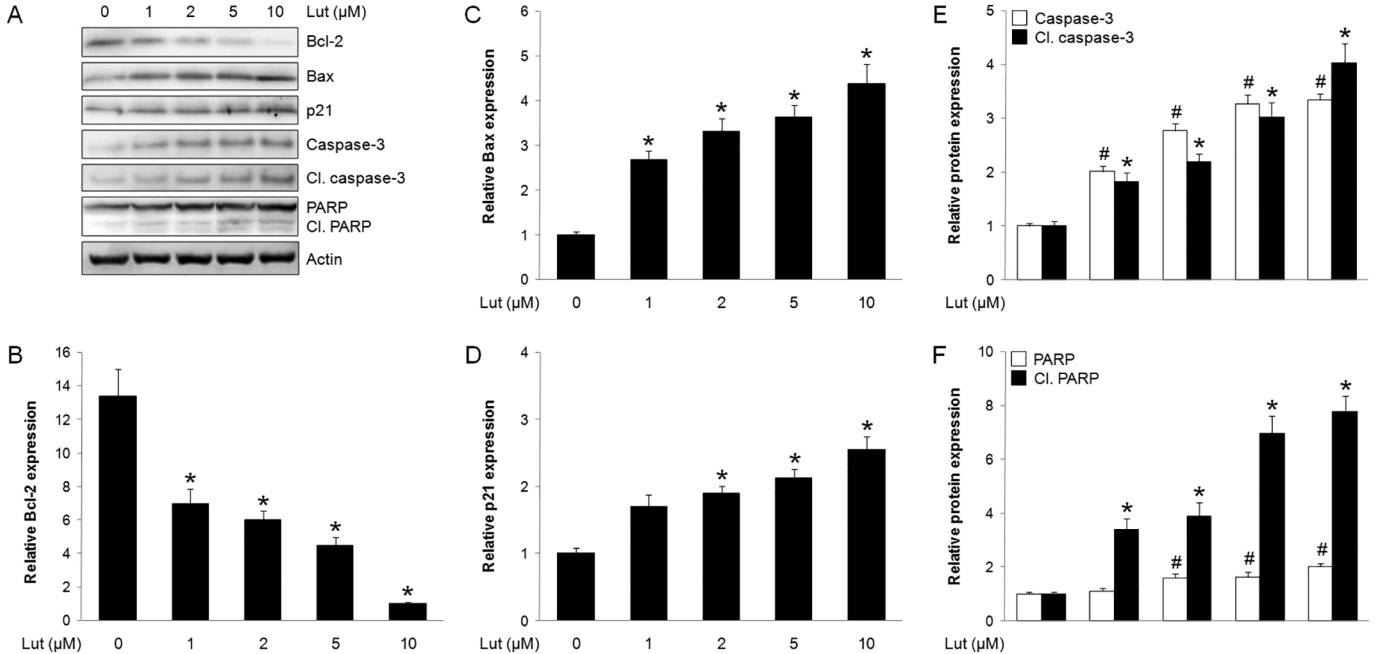
A
0 1 2 5 10 Lut (μM)
Bcl-2
Bax
p21
Caspase-3
Cl. caspase-3
PARP
Cl. PARP
Actin
B
Relative Bcl-2 expression
Lut (μM) 0 1 2 5 10
C
Relative Bax expression
Lut (μM) 0 1 2 5 10
D
Relative p21 expression
Lut (μM) 0 1 2 5 10
E
Caspase-3
Cl. caspase-3
Relative protein expression
Lut (μM)
F
PARP
Cl. PARP
Relative protein expression
Lut (μM)

Figure 4

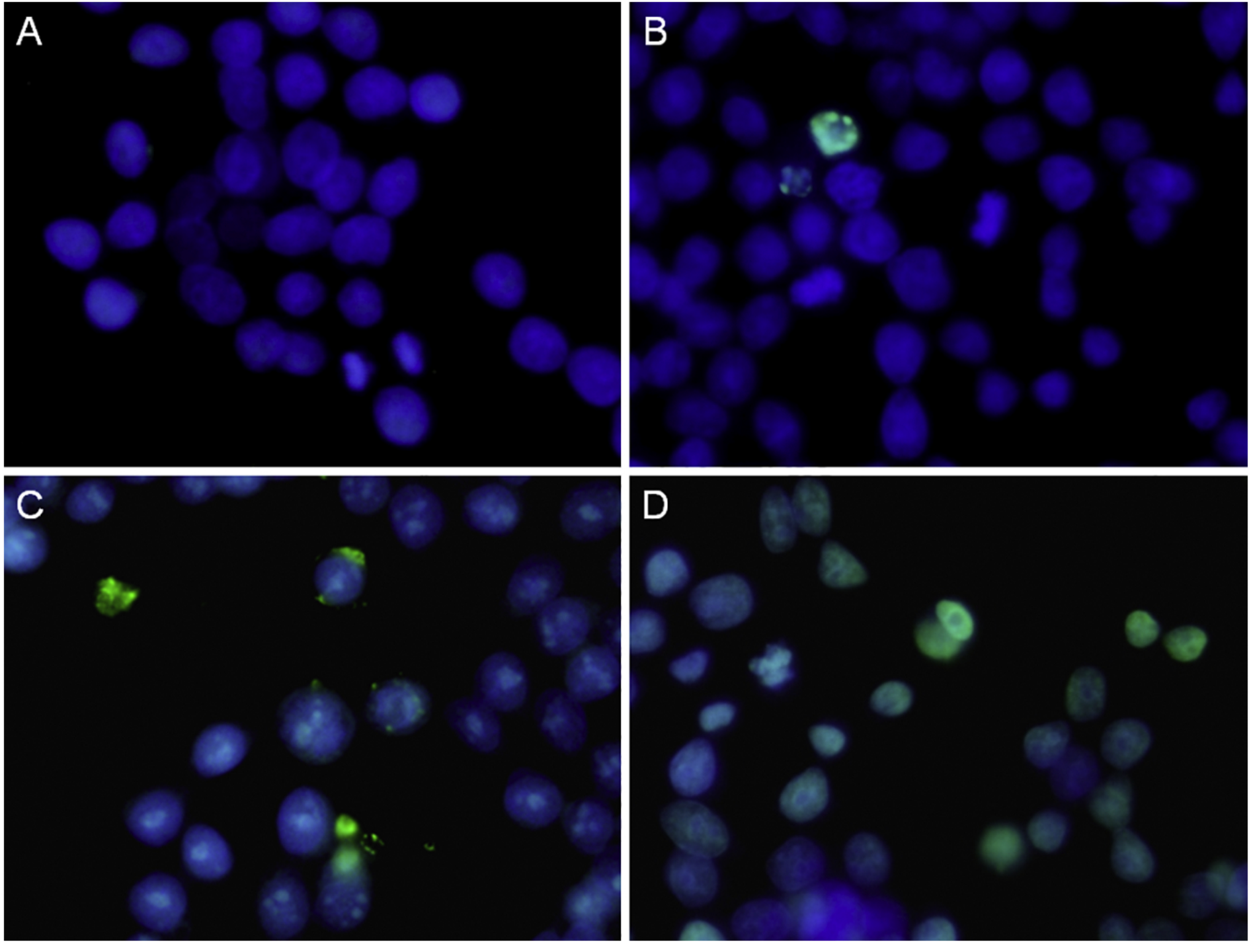

Figure 5

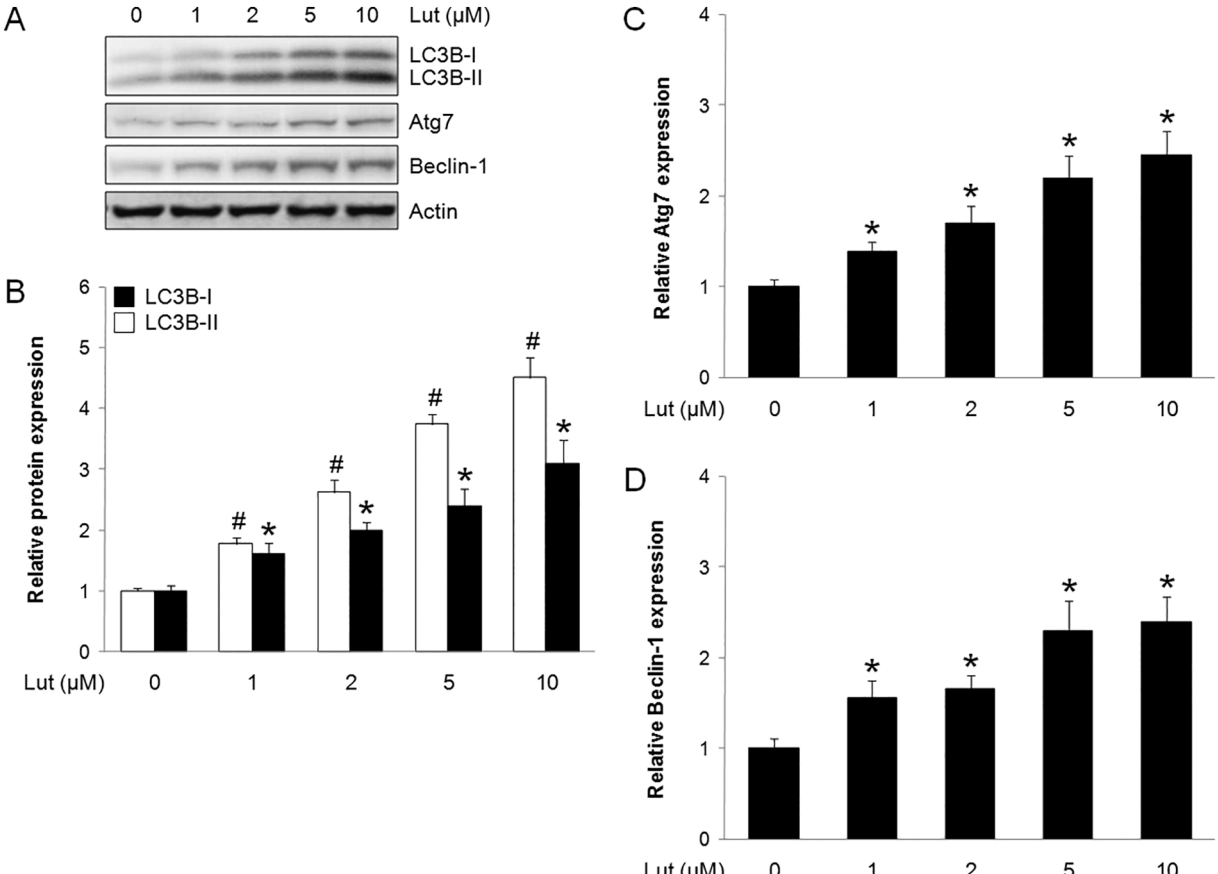
A
0
1
2
5
10
Lut (μM)
LC3B-I
LC3B-II
Atg7
Beclin-1
Actin
B
LC3B-I
LC3B-II
Relative protein expression
Lut (μM)
C
Relative Atg7 expression
D
Relative Beclin-1 expression

Figure 6

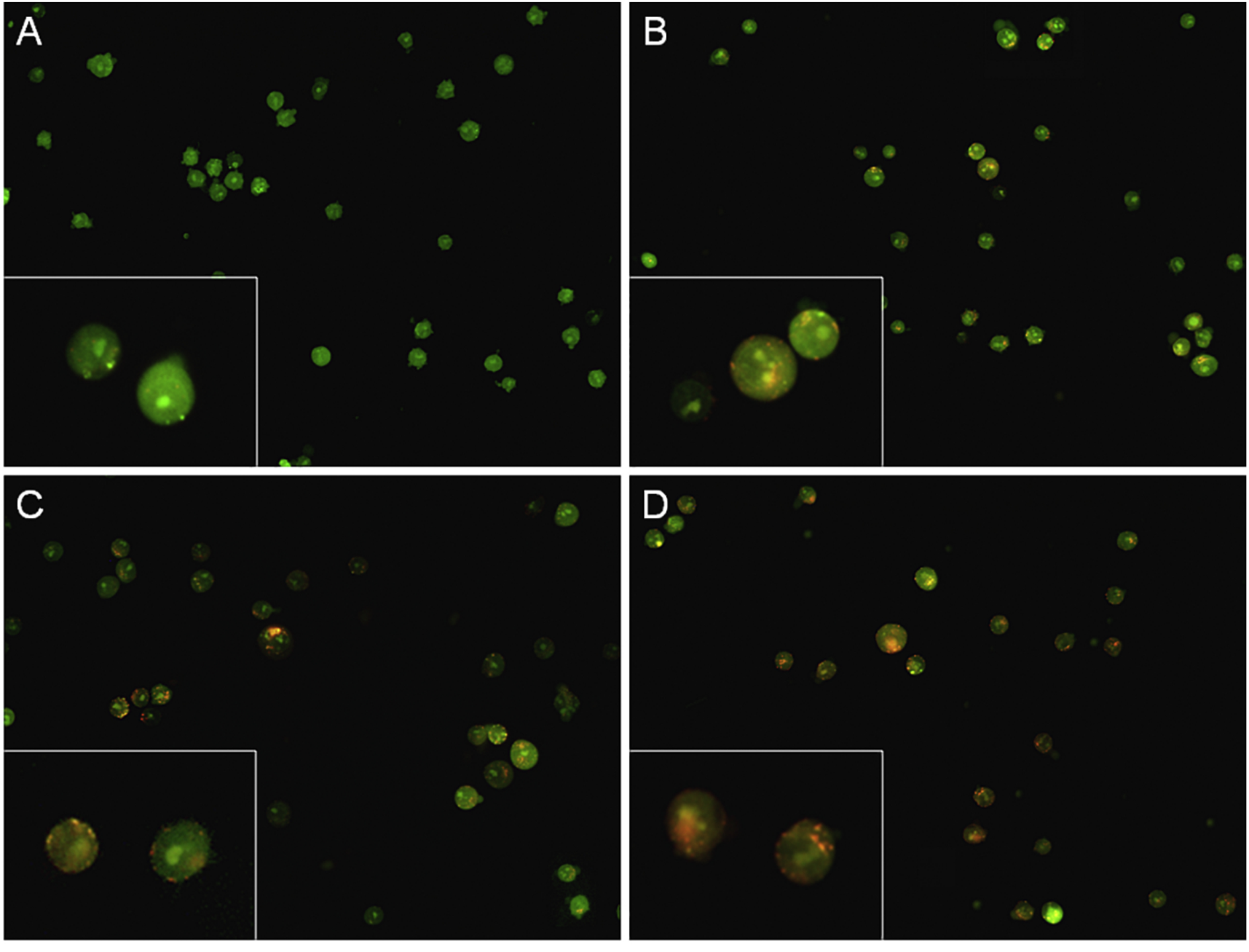

Figure 7

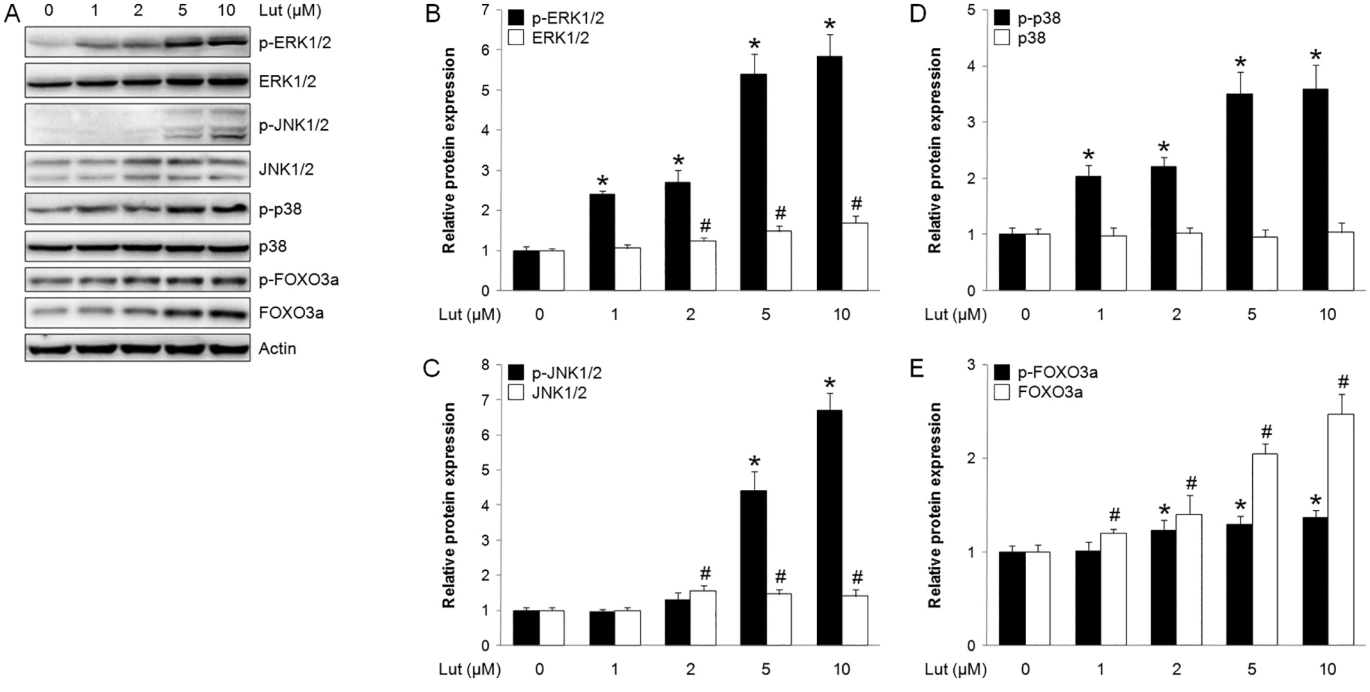
A
0
1
2
5
10
Lut (μM)
p-ERK1/2
ERK1/2
p-JNK1/2
JNK1/2
p-p38
p38
p-FOXO3a
FOXO3a
Actin
B
p-ERK1/2
ERK1/2
Relative protein expression
Lut (μM)
C
p-JNK1/2
JNK1/2
Relative protein expression
Lut (μM)
D
p-p38
p38
Relative protein expression
Lut (μM)
E
p-FOXO3a
FOXO3a
Relative protein expression
Lut (μM)

Figure 8

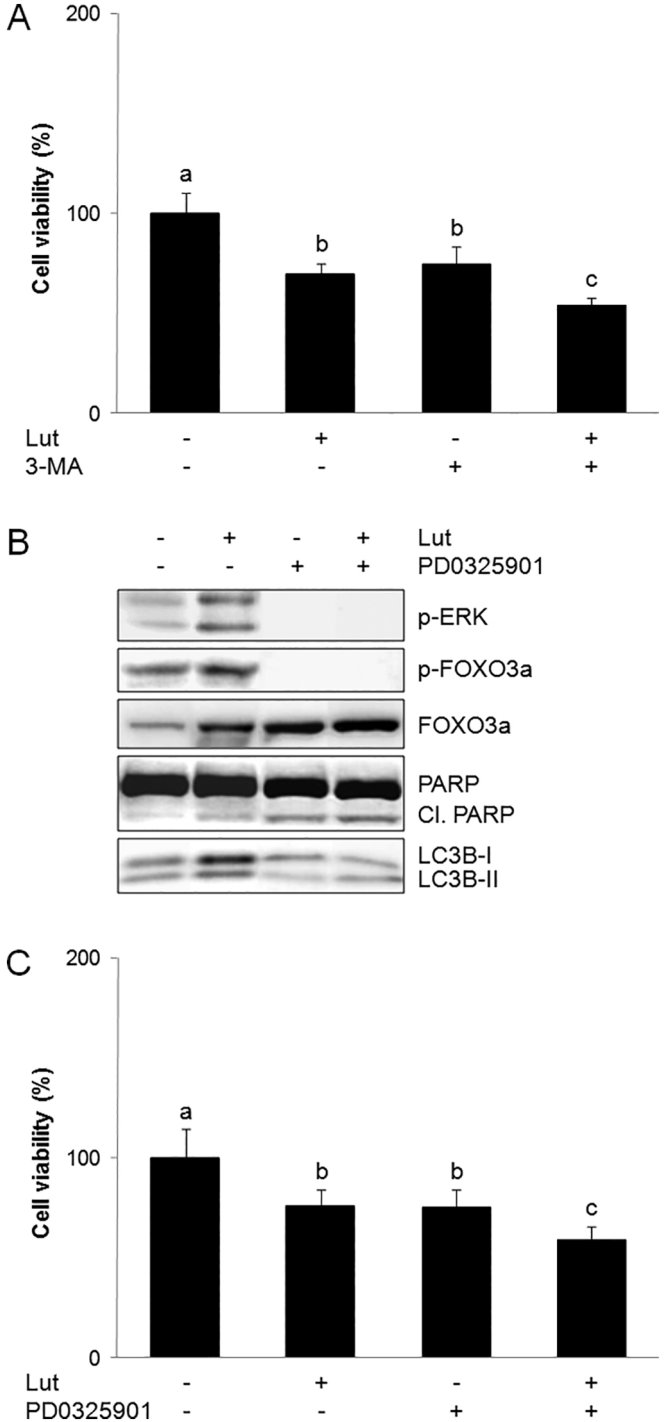
A
200
100
0
Cell viability (%)
a
b
b
c
Lut - + - +
3-MA - - + +
B
- + - + Lut
- - + + PD0325901
p-ERK
p-FOXO3a
FOXO3a
PARP
Cl. PARP
LC3B-I
LC3B-II
C
200
100
0
Cell viability (%)
a
b
b
c
Lut - + - +
PD0325901 - - + +

Figure 9

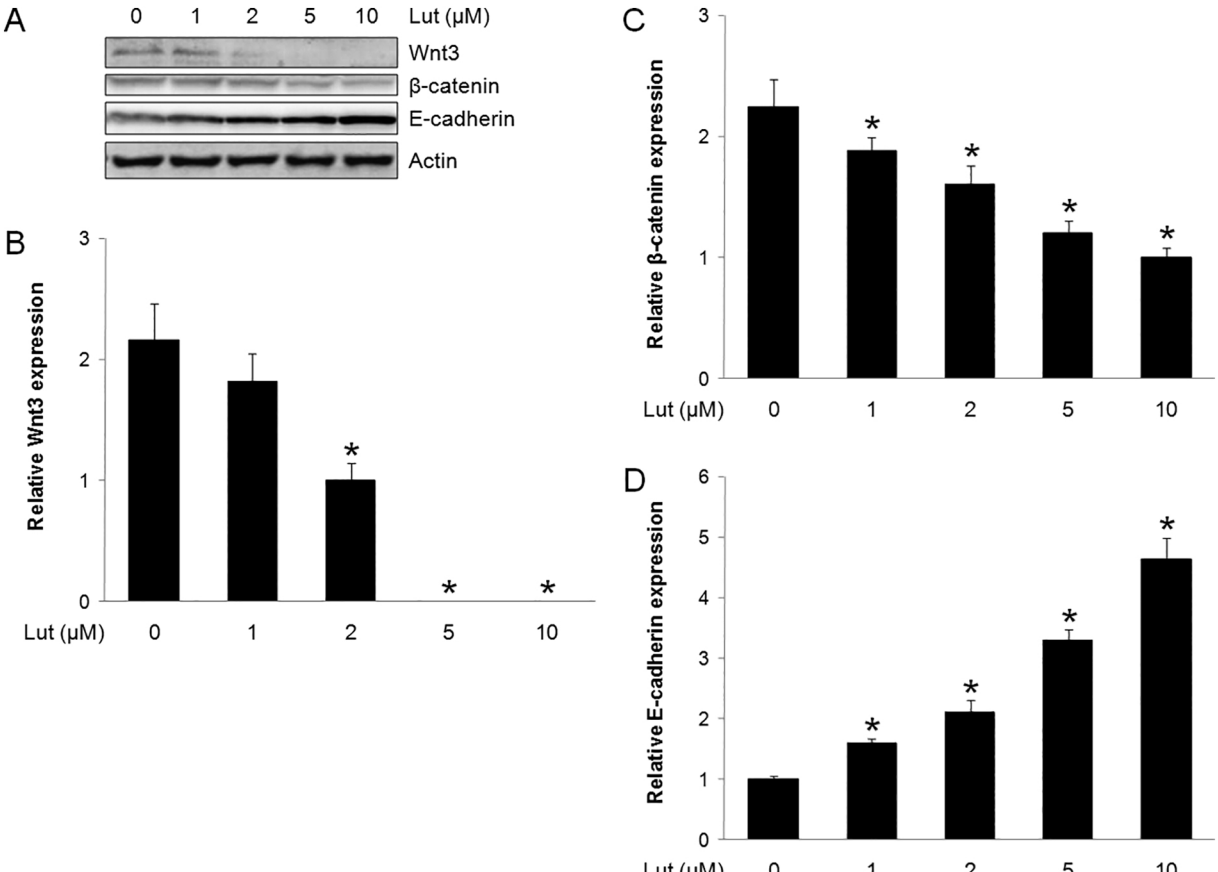
A
0
1
2
5
10
Lut (μM)
Wnt3
β-catenin
E-cadherin
Actin
B
Relative Wnt3 expression
3
2
1
0
*
*
Lut (μM)
0
1
2
5
10
C
Relative β-catenin expression
3
2
1
0
*
*
*
*
Lut (μM)
0
1
2
5
10
D
Relative E-cadherin expression
6
5
4
3
2
1
0
*
*
*
*
Lut (μM)
0
1
2
5
10

Figure 10